

Projectile charge dependence of electron emission from foils

Y. Sato, A. Higashi, and D. Ohsawa

National Institute of Radiological Sciences, 4-9-1 Anagawa, 263 Inage-Chiba, Japan

Y. Fujita, Y. Hashimoto, and S. Muto

KEK, 3-2-1 Midoricho, 188 Tanashi-Tokyo, Japan

(Received 19 May 1999; revised manuscript received 14 September 1999; published 3 April 2000)

We have precisely measured the secondary-electron-emission yield (γ) from thin Al, Ag, and Au foils with a thickness of $1\ \mu\text{m}$ on exposure to fully stripped $6\ \text{MeV}/n$ heavy ions (H, He, C, N, O, Ne, Si, and Ar). The dependence of the forward and backward yields on the projectile nuclear charge (z) showed a proportionality to the square of the effective charge (z_{eff}^2) and an oscillatory behavior with atomic number z ; the yields were comparatively low for exposures to He^{2+} and Ne^{10+} beams. The forward enhancement was significant for Al foil (light metal), depending on z ; in contrast, it was small for Ag and Au foils (heavy metals). The accuracy of the γ values was evaluated by determination of z_{eff} ($\pm 5\%$) and the surface reproducibility of the foil ($\pm 2\text{--}3\%$).

PACS number(s): 34.50.Bw, 34.50.Dy, 79.20.-m

I. INTRODUCTION

Sternglass [1] and several other authors [2–5] have shown theoretically that the ion-induced secondary-electron (SE) yield from thin foils, the well-known kinetic emission, is proportional to the stopping power in some atomic layers of the surface, and is a useful probe for studying the stopping power. In particular, the dependence on the effective charge of the projectiles (z_{eff}) of the SE yields from foils and their direction are of great interest from the viewpoints of atomic physics and radiobiology. For atomic numbers (z) ranging from proton to argon at several MeV/n (the Bragg-peak region), the stopping power is highly important from the viewpoint of heavy-ion therapy, and relevant SE data are greatly needed as useful information. There are, however, only a few data [6,7] in this energy region, which was the primary motivation for this work.

We have tried to measure precisely the z dependence of the SE yields from Al foil using fully stripped and fixed-velocity ($6\ \text{MeV}/n$) heavy-ion beams (H^+ , He^{2+} , C^{6+} , N^{7+} , O^{8+} , Ne^{10+} , Si^{14+} , and Ar^{18+}) from the NIRS-HIMAC Injector Linac [8]. After passing through a carbon stripper (thickness of $100\ \mu\text{g}/\text{cm}^2$) and two bending (20 deg and 70 deg) magnets, the magnetically analyzed beams were collected and transported to an experimental cave with a momentum spread of $\pm 0.25\%$ [9]. An energy of $6\ \text{MeV}/n$ corresponds to a projectile velocity of 15.1 a.u. ($\beta=0.11$), which is considered to be high enough to have no influence on the SE yields due to molecular processes or binding effects [10]. The charge effects on the SE yields can therefore be investigated in detail under the constant-velocity condition; this was the second motivation for our work.

Much effort was made to simplify and improve the apparatus in order to reduce the error in measurements down to the order of $\pm 2\text{--}3\%$. The ratio between the forward and backward yields is related to the combined influence of the projectile and target Coulomb fields (the well-known two-center effects); a fast (high-energy) electron experiences two separated Coulomb forces, suggesting a large forward SE

yield for the case of high- z projectiles. This ratio can thus be useful information not only to study the production of δ electrons, but also to improve and develop radiobiological models. In particular, good accuracy of the data is important for track-simulation studies, which have been actively carried out worldwide; this was an additional motivation for our study. In our case, the dominant uncertainty seems to have been due to the reproducibility of the surface condition of the foils ($\pm 2\text{--}3\%$) and the accuracy in calculating z_{eff} ($\pm 5\%$ at maximum), while the other errors were suppressed to below 1% in most cases. The dependence of the SE yields on the target materials was also measured using Ne^{10+} beams with three kinds of targets (commercially obtained Al, Ag, Au foils) with a thickness of $1\ \mu\text{m}$ were used. This paper reports principally on the precisely measured data of SE yields from Al foil from the viewpoints of the charge dependence, and the ratio between the forward (γ_F) and backward (γ_B) yields.

II. EXPERIMENT

The main apparatus used to measure the SE yields is schematically shown in Fig. 1. Three foils are used and the surrounding vacuum is 5×10^{-6} Torr; details of the apparatus and its application to fast detectors have already been presented in Ref. [11]. γ_F and γ_B are given by

$$\begin{aligned}\gamma_F &= z_{\text{eff}} Q_F / Q_z, \\ \gamma_B &= z_{\text{eff}} Q_B / Q_z,\end{aligned}\tag{1}$$

where Q_F and Q_B are the measured electron charges directly ejected forward and backward from a foil, respectively, and Q_z is the heavy-ion charge into the Faraday cup; since Q_z/z_{eff} corresponds to the number of heavy ions, each γ_F or γ_B is the mean number of ejected electrons per ion. We measured these negative-charge (electron) signals from both surfaces of the middle foil, which was biased at zero. A positive voltage (30 V) was directly supplied to both the

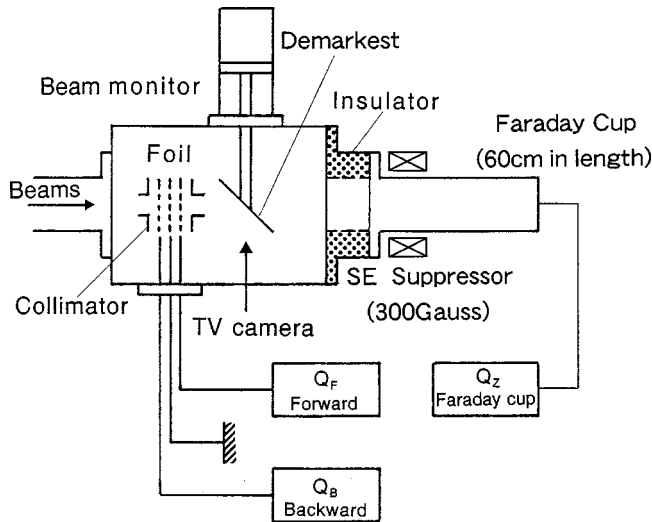


FIG. 1. Schematic drawing of the experimental setup. Three Al foils (effectively 40 mm^2 in area and $1 \mu\text{m}$ in thickness) are used with a gap of 2 mm. A permanent magnet (300 G) is placed at the entrance of the Faraday cup. Electrons are ejected from both surfaces of the middle foil, and are detected at both sides of the foils by using electrometers (Keithley 6517 A), which have an internal voltage source. [A fluorescent beam monitor (AF995R, Demarkest) is used to check the beam size.]

front and rear foils from an internal voltage source of two electrometers (Keithley 6517A). In this case the charge signal obtained from the rear foil corresponded to the forward SE yield (Q_F), and that from the front foil to the backward SE yield (Q_B). In other words, the emission from both surfaces of the middle foil was measured in two hemispherical directions, where each front or rear foil acted as a detector electrode. When passing through the first (front) foil, the beams should have reached their equilibrium charge state, because $1 \mu\text{m}$ ($300 \mu\text{g}/\text{cm}^2$) is thick enough to produce this condition; electron capture should have occurred only within the front foil. A correction of $(z - z_{\text{eff}})$ was thus made for γ_B , in such a way that the true γ_B was determined by adding $(z - z_{\text{eff}})$ to the measured value; this correction to the yield reached 2.6% at maximum for Ar.

At the outer sides of the three foils, two collimators (30 mm Φ in diameter, and with a brim) were equipped to produce an electric field similar to that in each foil gap (2 mm), and to prevent the escape of electrons (ejected from the foils) from this gap region in order to precisely measure Q_F and Q_B . These collimators (made of copper) are also effective to stop any halo beams produced upstream of the beam line as well as any stray electrons, resulting in a reduction of the error [11]. The size of the heavy-ion beam was always adjusted to around 5 mm Φ at a position of ± 1 mm on the fluorescent beam monitor just behind the foil (Fig. 1).

There is another scheme for more precisely measuring the SE yields, which is to indirectly measure a positive-charge signal from the middle foil when it is biased at a negative voltage; both sides of the foils are biased at zero. In this case the charge obtained (Q_T) is the same as the total SE yield from both surfaces of the middle foil, and is expected to be almost equal to the sum of Q_F and Q_B measured by the

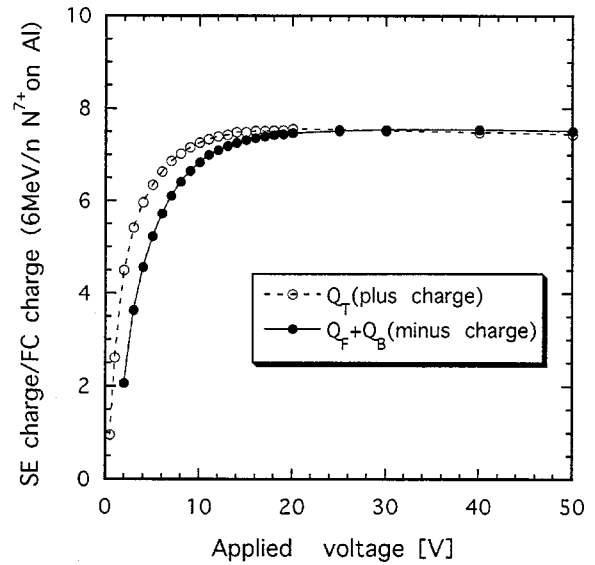


FIG. 2. Typical example of comparison between the total ejected-electron charge (plus, Q_T) and the detected-electron charge (minus, $Q_F + Q_B$) for N^{7+} vs the applied voltage (V). When V is larger than 20 V, a plateau can be seen.

previously mentioned scheme, though there is no information to distinguish the forward and backward yields. The difference between $(Q_F + Q_B)$ and Q_T was actually smaller than $\pm 1\%$ when the applied voltage was larger than 20 V (plateau region); in our configuration (Fig. 1) the area of each detector foil (40 mm^2) covered about 90% of the hemisphere (2π) in terms of the solid angle to the center axis of emission, and was large enough to collect most of the ejected electrons; a 2 mm gap corresponded to 10%. A typical example of a plateau curve for N^{7+} is shown in Fig. 2. The difference between Q_T and $Q_F + Q_B$ becomes large in the low-bias-voltage region; this is because the ejected electrons ($Q_F + Q_B$) from the detection electrode cannot return to the electrode because of the low electric field, thus having a small value in this case. Since the maximum energy of δ electrons should not exceed the order of several keV, most of them can stop within the detector foil (Al, $300 \mu\text{g}/\text{cm}^2$). This thickness seems to be nearly ‘‘thick’’ in the 6 MeV/n region, and a small difference in the thickness does not affect the yields [7]. Thus, the use of both an internal voltage source and the above-mentioned two collimators has allowed us to improve this kind of error. For determining γ_F and γ_B , the Q_F and Q_B values at an applied voltage of 30 V were used in this measurement. The error in Q_z was estimated to be below 1% [11].

There was a slight decrease in the energy (E) of the heavy-ion beams after passing through the foil, that is, their energy loss (ΔE) within the $1 \mu\text{m}$ foil; the SE yields should have been greater by about $\Delta E/E$. Incident heavy-ion beams passed through one sheet of Al foil for a measurement of Q_B , and two foils for Q_F . Q_B measured the emission from the front of the foil prior to significant energy loss in that foil, while Q_F measured the emission from the back after the ion had experienced essentially the full energy loss for that foil. The corresponding energy loss within a foil was evalu-

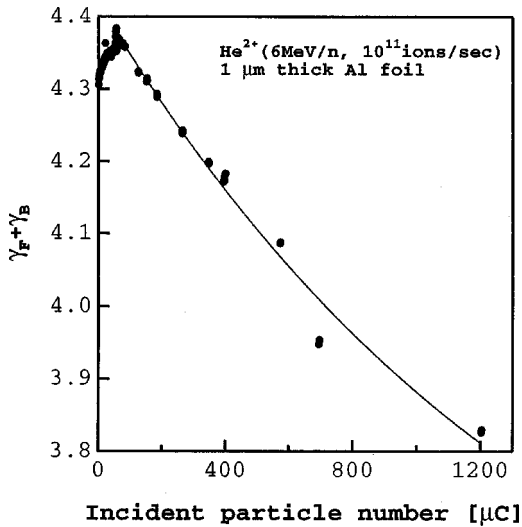


FIG. 3. Typical example of the SE yield vs total number of incident particles for He^{2+} . During the first few tens of minutes, the SE yield slightly increases and then reaches a maximum; after that, the yield decreases according to an approximately exponential curve. The measurement was carried out at around the peak of the curve, which corresponds to 100–200 μC for the case of He^{2+} . In this case the full-scale 1200 μC corresponds to a continuous irradiation time of about 10 h.

ated to be 66.0 keV when the foil was of pure Al, in the case of 6 MeV/n He^{2+} . Data for the stopping power (208 and 192 keV cm^2/mg for 22.5 and 25 MeV α particles) were taken from Ref. [12]. In the case of 24 MeV α particles, ΔE for 300 $\mu\text{g}/\text{cm}^2$ (1 μm thickness) Al is interpolated to be 66 keV. Thus the initial energy should be decreased by 0.3%, and the increase in the stopping power or SE yield is also of the same order. Although the ratio $\Delta E/E$ is 2% for the case of Ar^{18+} , it is still smaller than the error coming from the fluctuation in the surface condition. However, for the Q_F values (after two foils) of Si^{14+} and Ar^{18+} , the energy loss or increase in the SE yield reaches 3–4%; when considering these data at the energy of just 6 MeV/n, their γ_F values should be corrected to be lower by 3–4% than the actually measured ones. Among several errors in the measurement, the reproducibility (surface-dependent error) is dominant, and the effects from the energy loss are comparatively small, even for Q_F . The effects of nuclear reactions and recoil were negligible in this measurement, since their cross sections were very small compared to those of atomic collision in the energy region below 6 MeV/n.

The main problems in an Al foil are the oxidization and adsorption of other molecules (H_2O , N_2 , O_2 , and so on) on the surface. Although the details are unclear, such contamination effects were well studied using a model by Arrale *et al.* [13]; his results suggest our data are larger than a clean yield value by about 20% due to adsorption of residual gases under a vacuum of 5×10^{-6} Torr and an ion current density on the order of 10 nA/ cm^2 on the average. Judging from the measured characteristics of the SE yields ($\gamma_F + \gamma_B$) vs the total number of incident particles (Fig. 3), we estimate that the surface of the Al foil is a mixture of Al, Al_2O_3 , and some other molecules during the measurement, depending on the

number of irradiating particles and ion species. Our assumptions are as follows: (1) the surface of pure Al foil can generally be considered to be Al_2O_3 with some adsorption after it is exposed to the atmosphere for a while; (2) when the beam intensity is not very large and is on the order of 10^9 – 10^{11} pps, the surface of Al foil under vacuum conditions is nearly Al_2O_3 + [some other molecules (H_2O , O_2 , N_2)] at the beginning of exposure, and gradually changes to pure Al_2O_3 by sputtering as the total number of incident particles increases; (3) during the first exposure for a few tens of minutes, the SE yields slightly increase due to the reduction of such adsorbed molecules, which generally have a small stopping power compared to that of Al_2O_3 or Al; (4) adsorption and desorption reach an equilibrium state with each other, and the SE yields begin to gradually decrease by sputtering Al_2O_3 after about 30 min, according to an exponential curve; (5) after this point, the surface is changed from nearly pure Al_2O_3 to $\text{Al}_2\text{O}_3 + \text{Al}$. As can be seen in Fig. 3, the reduction of the yields reached 13% in 10 h, and had not yet saturated. This is because the difference in stopping power between Al and Al_2O_3 is on the order of several tens of percent; hence a decrease in the SE yields should finally be of the same order. Each yield measurement was for 20–30 min in duration to reduce the number of adsorbed molecules, and was performed within 1–1.5 h of the start of irradiation with a particular ion species, which means that the peak region ($\sim \text{Al}_2\text{O}_3$) of the curve (in Fig. 3) was used. In order to keep the foil conditions reasonably constant for various ion species, it was necessary to maintain an almost constant energy loss within the foils; the beam intensity was kept at between 10^9 and 10^{11} pps for H–Ar, depending on the ion species. The fluctuation rate during this short period (a few hours) could thus be evaluated to be smaller than 2% ($\pm 1\%$) for incident particles from protons to argon.

As mentioned above, the surface of the Al foils is actually close to Al_2O_3 with an equilibrium molecular density for all measurements in this work. When changing the foil, the fluctuation in Q_F and Q_B was largest, and reached \pm a few percent, depending on the individual surface conditions and ion species. The error in the measurement was thus evaluated to be $\pm 2\%$ in Q_F and Q_B for light ions and $\pm 3\%$ for ions heavier than Si.

III. RESULTS AND DISCUSSION

Figure 4 shows the relationship between z^2 and γ_F, γ_B , while Fig. 5 shows the two yields scaled by z_{eff}^2 (i.e., $Q_F/Q_z/z_{\text{eff}}$ and $Q_B/Q_z/z_{\text{eff}}$), in order to consider their correlation with the stopping power (the well-known Λ). The z_{eff} values were calculated using Ziegler's empirical formula [14], in which the accuracy is $\pm 5\%$ for z numbers of 6–92. For protons ($z=1$) and helium ($z=2$), this kind of accuracy is much better. Thus, the overall error in the SE yield (γ_F, γ_B) becomes about $\pm 6\%$ in both Figs. 4 and 5. These curves are roughly linear over a z range between 1 and 18; the best-fit results are $\gamma_F \propto z_{\text{eff}}^{1.92}$ and $\gamma_B \propto z_{\text{eff}}^{1.78}$. One can thus tell that the SE yield from foils is, to a first-order approximation, proportional to the stopping power; however, the yields for He^{2+} and Ne^{10+} are comparatively small, and the

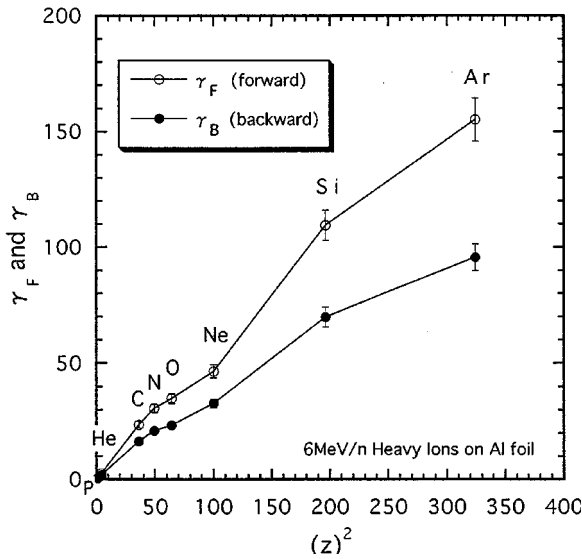


FIG. 4. γ_F and γ_B (forward and backward SE yields per ion) on Al vs z^2 with exposure to 6 MeV/n heavy ions. A reasonable proportionality, can be seen, though the yields have z oscillation and are comparatively small for He^{2+} and Ne^{10+} .

characteristics obviously have an oscillation, as first pointed out by Arrale *et al.* [15]. In Fig. 5 it is also possible to compare our data in this work with that of other experiments. Since there have been few other data on Al foils concerning γ_F in the several MeV/n region, only a comparison of γ_B is possible. Since the detailed distribution of the charge fraction in each z_{eff} is not well known, the z_{eff}^2 values were calculated using the z_{eff} values obtained by Ziegler's formula; the possible error involved in such a calculation, however, is smaller than 1%.

The following is a comparison between our data and some others under similar vacuum conditions (5×10^{-6} Torr in our

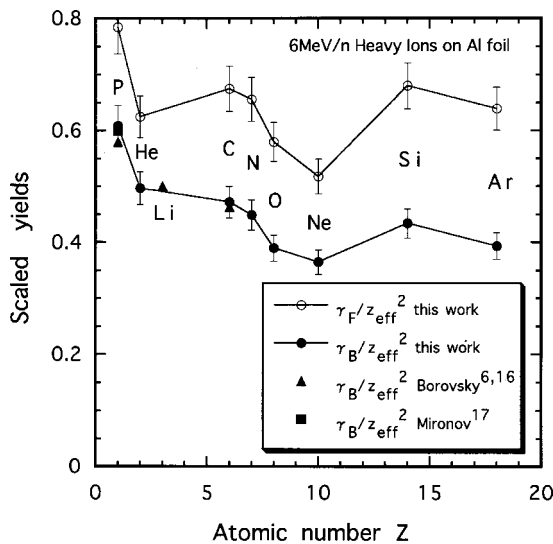


FIG. 5. γ_F and γ_B per z_{eff}^2 on Al vs z with exposure to 6 MeV/n heavy ions ($\gamma_F \propto z_{\text{eff}}^{1.92}$ and $\gamma_B \propto z_{\text{eff}}^{1.78}$). Some other data (H^+ , Li^{3+} , C^{6+}) are also plotted, and z oscillation can be clearly seen.

case). From the experiments of Borovsky *et al.* ($\sim 10^{-5}$ Torr), the value for a 6 MeV proton on Al_2O_3 can be precisely interpolated to be $\gamma_B = 0.58$ from several data points over 5–24 MeV [16]; from the early data of Mironov and Nemenov, the value is about 0.6 [17]. These two values agree well with our data ($0.609 \pm 2\%$). Meanwhile, only the data of Castaneda *et al.* [18] (protons and α particles on Al_2O_3 at $\sim 10^{-6}$ Torr) show a considerably small value (0.45 for 6 MeV protons) compared with other data; in his case, the surface may have been rather clean under a good vacuum. From the heavy-ion data of Borovsky and Barraclough ($\sim 10^{-5}$ Torr) [6], γ_B of ${}^7\text{Li}^{3+}$ on Al_2O_3 can be extrapolated to be 4.5 at 6 MeV/n (42 MeV), which corresponds to 0.5 for $\gamma_B/z_{\text{eff}}^2$, as plotted in Fig. 5. The calculated value (γ_B) of 16.3 for C^{6+} on Al_2O_3 using the semiempirical equation of [6] corresponds to 0.46 for $\gamma_B/z_{\text{eff}}^2$, and agrees well with our 6 MeV/n C^{6+} data ($0.472 \pm 6\%$). His actual C^{6+} value of 16.0 at 63 MeV (5.25 MeV/n) is also comparable with our data. Figure 5 also shows a gradual decrease in the curve of $\gamma_B/z_{\text{eff}}^2$ along with an increase in z (γ_B is roughly proportional to $z_{\text{eff}}^{1.78}$); a similar tendency with 6.2 MeV/n He^{2+} , N^{7+} , and O^{8+} was presented in the experiment of Koyama *et al.* with Au foil [19] and that of Rothard *et al.* with C foil [7], in which the ratio of γ_B for projectiles between proton and Ne is 50–60%, and is similar to the curve in Fig. 5. The γ_B values obtained in this work are thus quite consistent with other data.

As previously mentioned, two or three valleys can be seen in the two curves (γ_F and γ_B) in Fig. 5. The forward yield with protons is larger than that with He^{2+} by 25%. After that, the yield gradually decreases and reaches a minimum for the Ne^{10+} beam; the difference between C^{6+} (or Si^{14+}) and Ne^{10+} is 30–31%. The yield with Ar^{18+} is smaller than that with Si^{14+} by 6%. It is thus clear that the yields have z oscillation. This tendency appears to be somewhat clear in the forward direction, and is similar to the data of Arrale *et al.* [15]; the oscillation seems to be related to the production mechanism of δ electrons or the behavior of two-center effects. γ_B is somewhat small at $z=4$ and 24 in Rothard *et al.*'s data [7], and at $z=2$ and 10 in Fig. 5, suggesting that z oscillation depends on the target materials. As can be seen from Fig. 5, Borovsky *et al.*'s data for H^+ , Li^{3+} , and C^{6+} on Al [6,16] may have already suggested such a tendency. Also, Castaneda *et al.*'s data [18] show a similar tendency, in which the yields with 4.5 and 6.35 MeV/n deuteron beams are higher than those with the same-velocity α particles by 21% and 9%, respectively. For such z oscillation, screening effects by target electrons in a continuum state may play an important role [20].

The ratio (R) of γ_F/γ_B (Q_F/Q_B in our case) has also been evaluated. For Al foil (light material), a large forward enhancement and its dependence on z can be observed in Fig. 6, which is similar to the recent data of Rothard *et al.* on C foil [7]. These results suggest that many electrons initially ejected in the backward direction are pulled by the strong Coulomb field of a highly charged projectile, and some of them are deflected into the forward direction with high energy, as discussed in [10,21]. The data of Rothard *et al.* [22]

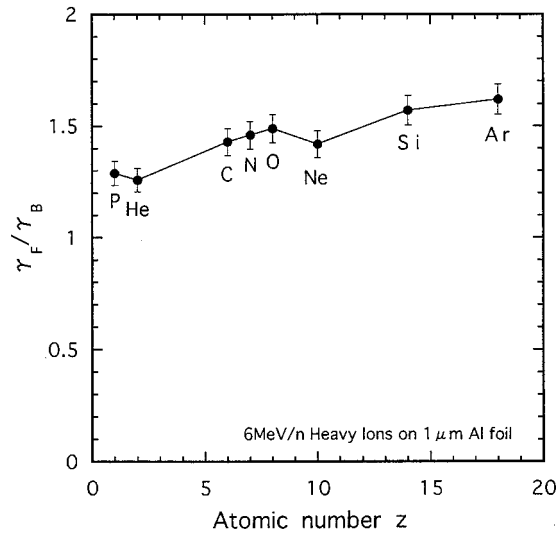


FIG. 6. Ratio between γ_F and γ_B for 6 MeV/n heavy ions on Al foil vs z .

show that R is 1.13–1.37 for He–Ar on Al foil, which is smaller than the values of this work (1.26–1.62 in Fig. 6) by 12–18%. This difference might be because the beams were not highly charged and the projectile velocities were low (≤ 600 keV/n) in the experiment of [22] resulting in a low equilibrium charge state (weak Coulomb field) within the target.

For heavy-metal foils (Ag and Au), however, the forward and backward yields were almost identical; comparisons of each yield with Ne^{10+} are given in Fig. 7. As can also be seen in Fig. 7, γ_B depends slightly on the target atomic number, while γ_F is almost constant. These two results suggest that (1) a sufficient relaxation of high-energy electrons occurs within dense materials, resulting in isotropic emission from the surface of heavy-metal foils and (2) the target dependence is consequently small.

IV. SUMMARY

Data for the SE yields from Al foil (Fig. 4) have been obtained with an overall error of $\pm 6\%$ for bare projectiles from proton to argon under a 6 MeV/n fixed-velocity condi-

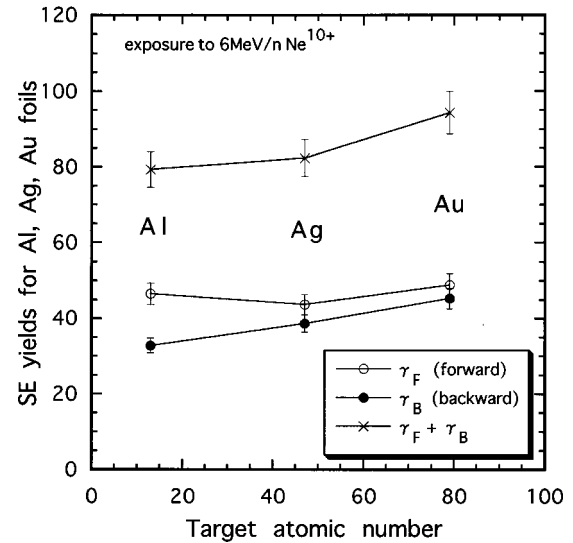


FIG. 7. γ_F and γ_B on Al, Ag, and Au vs atomic number with exposure to 6 MeV/n Ne^{10+} beams. The ratio between γ_F and γ_B is large for Al (light material), though it is small for Ag and Au (heavy materials).

tion, for both the forward and backward directions. The surface of the Al foils should have been nearly Al_2O_3 with an equilibrium molecular density throughout the experiments. The accuracy of the data was determined mainly by that in the calculation of $z_{\text{eff}}(\pm 5\%)$ and the error in the measurement ($\pm 2\text{--}3\%$). The charge dependence was shown to be roughly proportional to z_{eff}^2 along with z oscillation. Even in the vacuum used (5×10^{-6} Torr), it was possible to precisely measure the projectile charge (z) dependence of the electron emission. An improvement in the base vacuum by 3–4 orders of magnitude and sufficient sputtering will allow us to obtain more detailed information from a clean surface.

ACKNOWLEDGMENTS

The authors would like to thank Dr. F. Soga and Dr. T. Fujisawa for fruitful discussions on atomic physics. This work was part of the Research Project with Heavy Ions at NIRS-HIMAC (Heavy Ion Medical Accelerator) in Chiba, which is supported by the Science and Technology Agency of Japan.

-
- [1] E. J. Sternglass, Phys. Rev. **108**, 1 (1957).
 - [2] H. Rothard, J. Schou, and K. O. Groeneveld, Phys. Rev. A **45**, 1701 (1992).
 - [3] A. Clouvas, H. Rothard, M. Burkard, K. Kroneberger, C. Biedermaier, J. Kemmler, and K. O. Groeneveld, Phys. Rev. B **39**, 6316 (1989).
 - [4] M. Burkard, H. Rothard, J. Kemmler, K. Kroneberger, and K. O. Groeneveld, J. Phys. D **21**, 472 (1988).
 - [5] O. Benka, A. Schinner, T. Fink, and M. Pfaffenlehner, Phys. Rev. A **52**, 3959 (1995).
 - [6] J. E. Borovsky and B. L. Barraclough, Nucl. Instrum. Methods Phys. Res. B **36**, 377 (1989).
 - [7] H. Rothard, M. Jung, M. Caron, J.-P. Grandin, B. Gervais, A. Billebaud, A. Clouvas, and R. Wunsch, Phys. Rev. A **57**, 3660 (1998).
 - [8] Y. Sato, A. Kitagawa, H. Ogawa, and S. Yamada, J. Appl. Phys. **76**, 3947 (1994).
 - [9] Y. Sato, A. Tanaka, Y. Furusawa, S. Matsumoto, T. Murakami, F. Soga, K. Takeo, and Y. Fujita, Rev. Sci. Instrum. **67**, 2000 (1996).
 - [10] D. Schneider, D. DeWitt, A. S. Schlachter, R. E. Olson, W. G. Graham, J. R. Mowat, R. D. DuBois, D. H. Loyd, V. Montemayor, and G. Schwietz, Phys. Rev. A **40**, 2971 (1989).
 - [11] Y. Fujita, Y. Hashimoto, S. Muto, A. Higashi, Y. Sato, D.

- Ohsawa, and F. Soga (unpublished).
- [12] ICRU Report No. 49, 1993 (unpublished), pp. 192, 214.
- [13] A. M. Arrale, Z. Y. Zhao, J. F. Kirchoff, D. K. Marble, D. L. Weathers, F. D. McDaniel, and S. Matteson, Nucl. Instrum. Methods Phys. Res. B **89**, 437 (1994).
- [14] J. F. Ziegler, Nucl. Instrum. Methods **168**, 17 (1980).
- [15] A. M. Arrale, Z. Y. Zhao, J. F. Kirchoff, D. L. Weathers, F. D. McDaniel, and S. Matteson, Phys. Rev. A **55**, 1119 (1997).
- [16] J. E. Borovsky, D. J. McComas, and B. L. Barraclough, Nucl. Instrum. Methods Phys. Res. B **30**, 191 (1988).
- [17] E. S. Mironov and L. M. Nemenov, Zh. Eksp. Teor. Fiz. [Sov. Phys. JETP] **5**, 188 (1957).
- [18] C. M. Castaneda, L. McGarry, C. Cahill, and T. Essert, Nucl. Instrum. Methods Phys. Res. B **129**, 199 (1997).
- [19] A. Koyama, T. Shikata, H. Sakairi, and E. Yagi, Jpn. J. Appl. Phys., Part 1 **21**, 1216 (1982).
- [20] C. M. Fey, G. Dollinger, A. Bergmaier, T. Faestermann, and P. Maier-Komor, Nucl. Instrum. Methods Phys. Res. B **99**, 205 (1995).
- [21] N. Stolterfoht, D. Schneider, J. Tanis, H. Altevogt, A. Salin, P. D. Fainstein, R. Rivarola, J. P. Grandin, J. N. Scheurer, S. Andriamonje, D. Bertault, and J. F. Chemin, Europhys. Lett. **4**, 899 (1987).
- [22] H. Rothard, K. Kroneberger, A. Clouvas, E. Veje, P. Lorenzen, N. Keller, J. Kemmler, W. Meckback, and K. O. Groeneveld, Phys. Rev. A **41**, 2521 (1990).